JOURNAL OF AIRCRAFT
Vol. 33, No. 5, September–October 1996

Unsteady Aerodynamics of a Flapped Airfoil in Subsonic Flow by Indicial Concepts

Nagarajan Hariharan* and J. Gordon Leishman†
University of Maryland, College Park, Maryland 20742

An approach based on indicial concepts is described to model the unsteady airloads on a thin airfoil in subsonic compressible flow caused by the arbitrary motion of a trailing-edge flap. Exact indicial aerodynamic responses at small values of time as a result of flap deflection and angular deflection rate about the flap hinge are obtained from linear unsteady subsonic theory in conjunction with the aerodynamic reverse flow theorems. Using the known exact initial (piston theory) and asymptotic values of the airloads, along with an assumed analytic form for the indicial functions, these exact results are used to help obtain complete approximations for the respective indicial responses. The airloads from arbitrary flap motion in subsonic flow are subsequently obtained in state-space form. Validation of the method is conducted with experimental data for time-dependent flap motions.

Nomenclature

A_i = coefficients of indicial functions
a = pitch axis location, semichords
a_s = sonic velocity, ms^{-1}
b = semichord, $c/2$, m
b_i = exponents of indicial functions
C_D = pressure drag coefficient
C_F = flap force coefficient
C_H = flap hinge moment coefficient
C_M = moment coefficient about one-quarter-chord
C_N = normal force coefficient
C_p = pressure coefficient
C_S = leading-edge suction force coefficient
c = airfoil chord, $2b$, m
e = flap hinge location, semichords
F_1–F_{20} = geometric constants for flap
f = flap oscillation frequency
H = hinge moment, N m
K = noncirculatory time constant
M = Mach number
N = normal force, N
S = distance traveled in semichords, $2Vt/c$
T = noncirculatory time constant in S time
T' = noncirculatory time constant in t time
T_i = basic noncirculatory time constant, c/a_s
t = time, s
$\hat{t}$ = nondimensional time
V = freestream velocity, ms^{-1}
x = airfoil chord axis (origin at midchord), m
z = state variable
α = angle of attack, rad
β = Glauert compressibility factor, $\sqrt{1-M^2}$
Δ = incremental quantity
δ = flap deflection angle, rad
ε_N, ε_M, ε_H = flap effectiveness factors
η = leading-edge suction force recovery factor
ϕ = indicial response function

Subscripts
eff = effective component
H = hinge moment component
M = moment component
N = normal force component
qs = quasisteady component
α = angle-of-attack component
$\dot{\alpha}$ = pitch rate component
δ = flap deflection angle component
$\dot{\delta}$ = flap deflection rate component

Superscripts
c = circulatory component
f = flap component
i = noncirculatory (impulsive) component

Introduction

THERE have been several applications of a wing-based trailing-edge flap applied to gust alleviation or flutter suppression on fixed-wing aircraft.[1,2] However, for helicopters the use of flaps on the rotor blades has, so far at least, found use only for collective and one/revolution cyclic pitch control. Today, with the advent of lightweight smart materials–structures and high bandwidth active control technologies, it is now becoming increasingly feasible to use compliant airfoil surfaces or trailing-edge mounted flaps on the rotor blades as a means of individually controlling the aerodynamic environment on each blade, and at frequencies much higher than one/revolution. This offers tremendous possibilities for reducing blade loads and vibration levels.[3]

Recent results from smart structures and materials research have shown that individual blade lift control is possible on a Froude-scale helicopter rotor by means of a small outboard trailing-edge flap controlled by piezoceramic actuators.[4] In another experiment, a mechanically actuated flap system provided evidence that the flap can help reduce rotor noise.[5] Parallel theoretical studies of these problems using advanced helicopter rotor models[6,7] require the use of a suitably formulated time-domain theory for the blade section aerodynamics. An unsteady aerodynamic theory is required, firstly because the local actuation rate may be very high, and secondly, be-

Presented, in part, as Paper AIAA 95-1228 at the AIAA/ASME/ASCE/AHS/ASC 36th Structures, Structural Dynamics, and Materials Conference, April 10–12, 1995, New Orleans, LA; received July 16, 1995; revision received April 11, 1996; accepted for publication April 15, 1996.

*Graduate Research Assistant, Center for Rotorcraft Education and Research, Glenn L. Martin Institute of Technology, Department of Aerospace Engineering; currently Member, Technical Staff, Department of Advanced Systems, SETA Corporation, McLean, VA 22101.

†Associate Professor, Center for Rotorcraft Education and Research, Glenn L. Martin Institute of Technology, Department of Aerospace Engineering. Senior Member AIAA.

cause high-resolution predictions of acoustics need to be made. In addition, since the local effective reduced frequencies based on active camber motion may exceed unity, incompressible assumptions may no longer be adequate.

The objective of this article is to describe the development of an unsteady aerodynamic theory for the effects of a trailing-edge flap based on indicial function concepts. The work is an extension to that originally reported in Ref. 8. The results can be generalized to any form of chordwise camber, but the analysis presented here is restricted only to the trailing-edge flap problem. The method is formulated in the spirit of classical unsteady subsonic airfoil theory, where the assumptions are that the problem is governed by the linearized partial differential equation and linearized boundary conditions. The two-dimensional solution described in this article is assumed to be representative of the environment encountered by a rotor blade element; the effects of the trailed wake being accounted for by means of an additional inflow angle in the conventional way. Furthermore, it will be assumed that the freestream velocity or Mach number is quasisteady, although the results can also be extended to time-varying freestreams, and the procedures are outlined in Ref. 9. Finally, the method reported in this article is developed in a computational form suitable for use in routine rotor loads and aeroelasticity applications, and therefore, includes some additional assumptions and approximations to make the method practical.

Methodology

Incompressible Flow

The prediction of unsteady lift, airfoil pitching moment, and the hinge moment on an airfoil for a harmonic flap oscillation in incompressible flow has been studied.[10-12] The complete expressions for the unsteady lift in the frequency domain, from both airfoil motion and flap oscillation, were systematically obtained in terms of contributions from noncirculatory (apparent mass) and circulatory terms (shed-wake effects). Validation of the incompressible unsteady thin airfoil theory with a flap has been made by Drescher.[13]

Numerical methods for the unsteady aerodynamics caused from arbitrary motion can be derived by the use of Duhamel superposition with the Wagner indicial (step) response. The Wagner function, like the Theodorsen function, is known exactly. However, for practical evaluations of the aerodynamics an exponential approximation is usually used since this facilitates straightforward manipulation by Laplace transforms.[14] Using this convenient exponential approximation the aerodynamic transfer functions can be obtained, and the unsteady forces and moments caused by arbitrary motion can be cast into state–space[15,16] or one-step recursive forms.[17,18]

For arbitrary trailing-edge flap motion the airloads can be written in a similar numerical form, with the total airloads found by linear superposition. The complete aerodynamic system for the airfoil and flap in an incompressible flow can be represented by a set of four aerodynamic states.[8,19,20] Although it is convenient for some purposes to separate out the circulatory lift from airfoil motion to that from the flap motion, in a practical application their net effects can be combined so that, in fact, only two states are required to model the circulatory part of the unsteady airloads in incompressible flow. The inclusion of gust effects, however, adds two more states because a different indicial function applies.

Subsonic Flow

There are no equivalent exact results analogous to Theodorsen's theory or Wagner's solution for the unsteady subsonic compressible flow case. Under these conditions both the circulatory and the noncirculatory loads have time–history effects; unlike incompressible flow the noncirculatory loads are no longer proportional to the instantaneous airfoil and flap displacements since they are related to the propagation and reflection of wave disturbances. This means the noncirculatory terms must also be described by aerodynamic states. A solution starting from the indicial response is desired for the subsonic problem because it is known that this permits a generalization to arbitrary forcing by means of Duhamel superposition. However, while the initial ($S = 0$) and final ($S = \infty$) values of the indicial response are known exactly in linearized subsonic flow, the intermediate behavior is known exactly only for very limited values of time.

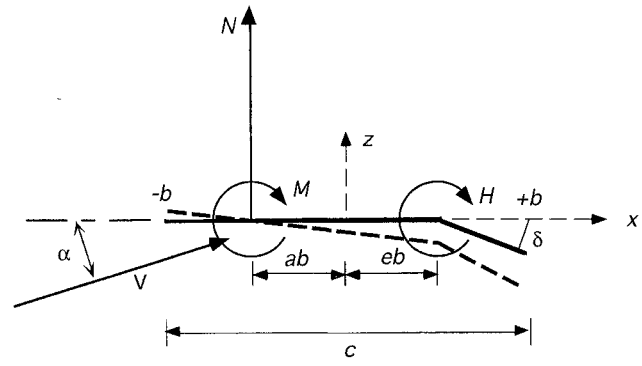

Fig. 1 Nomenclature for thin airfoil with a trailing-edge flap.

Initial and Final Values of Indicial Response

As explained by Lomax[21] the initial airloading on an airfoil operating in a compressible flow in response to a step change in the boundary condition is associated with the acoustic wave system created by the initial perturbation. The airloading at time zero ($S = 0$) can be computed directly using piston theory, and the results for the airfoil case have been given previously.[14,21-23] For indicial flap motion about a hinge located at *eb* (see Fig. 1) the initial airloads are

$$\Delta C_{N_\delta}(S = 0, M) = [2(1 - e)/M]\Delta\delta \tag{1}$$

$$\Delta C_{N_{\dot\delta}}(S = 0, M) = [(1 - e)^2/2M]\Delta(\dot\delta c/V) \tag{2}$$

$$\Delta C_{M_\delta}(S = 0, M) = -[(1 - e)(2 + e)/2M]\Delta\delta \tag{3}$$

$$\Delta C_{M_{\dot\delta}}(S = 0, M) = -(1/12M)[(1 + e)^3 - (12e - 4) - \tfrac{3}{2}(1 - e)^2]\Delta(\dot\delta c/V) \tag{4}$$

$$\Delta C_{H_\delta}(S = 0, M) = -[(1 - e)^2/2M]\Delta\delta \tag{5}$$

$$\Delta C_{H_{\dot\delta}}(S = 0, M) = -[(1 - e)^3/6M]\Delta(\dot\delta c/V) \tag{6}$$

These results are valid for any M, but only at the instant in time when the perturbation (δ or $\dot\delta c/V$) is applied.

The final values of the indicial response are given by the usual linearized subsonic theory, so that for indicial flap displacements and rates

$$\Delta C_{N_\delta}(S = \infty, M) = \frac{2F_{10}}{\beta}\Delta\delta \tag{7}$$

$$\Delta C_{N_{\dot\delta}}(S = \infty, M) = \frac{F_{11}}{2\beta}\Delta\left(\frac{\dot\delta c}{V}\right) \tag{8}$$

$$\Delta C_{M_\delta}(S = \infty, M) = -\frac{F_4 + F_{10}}{2\beta}\Delta\delta \tag{9}$$

$$\Delta C_{M_{\dot\delta}}(S = \infty, M) = -\frac{2F_1 - 2F_8 - (2e + 1)F_4 + F_{11}}{8\beta}\Delta\left(\frac{\dot\delta c}{V}\right) \tag{10}$$

$$\Delta C_{H_\delta}(S = \infty, M) = -\frac{(F_5 - F_4F_{10}) + F_{12}F_{10}}{2\pi\beta}\Delta\delta \quad (11)$$

$$\Delta C_{H_{\dot\delta}}(S = \infty, M) = -\frac{F_{11}(F_{12} - F_4)}{4\pi\beta}\Delta\left(\frac{\dot\delta c}{V}\right) \quad (12)$$

where the F coefficients are defined by Theodorsen[11] and are also listed in Refs. 19 and 20.

Approximations to Indicial Airloads

The intermediate indicial behavior between $S = 0$ and $S = \infty$ must now be defined. Following Ref. 8, the indicial lift, airfoil moment, and hinge moment coefficients as a result of impulsive flap deflection can be written in general functional form as

$$\Delta C_{N_\delta}(S, M, e) = \left[\frac{2(1 - e)}{M}\phi^i_{N_\delta}(S, M, e) + \frac{2F_{10}}{\beta}\phi^c_{N_\delta}(S, M, e)\right]\Delta\delta \quad (13)$$

$$\Delta C_{N_{\dot\delta}}(S, M, e) = \left[\frac{(1 - e)^2}{2M}\phi^i_{N_{\dot\delta}}(S, M, e) + \frac{F_{11}}{2\beta}\phi^c_{N_{\dot\delta}}(S, M, e)\right]\Delta\left(\frac{\dot\delta c}{V}\right) \quad (14)$$

$$\Delta C_{M_\delta}(S, M, e) = -\left[\frac{(1 - e)(2 + e)}{2M}\phi^i_{M_\delta}(S, M, e) + \frac{F_4 + F_{10}}{2\beta}\phi^c_{M_\delta}(S, M, e)\right]\Delta\delta \quad (15)$$

$$\Delta C_{M_{\dot\delta}}(S, M, e) = -\left\{\frac{1}{12M}\left[(1 + e)^3 - (12e - 4) - \frac{3}{2}(1 - e)^2\right]\phi^i_{M_{\dot\delta}}(S, M, e) + \frac{2F_1 - 2F_8 - (2e + 1)F_4 + F_{11}}{8\beta}\phi^c_{M_{\dot\delta}}(S, M, e)\right\}\Delta\left(\frac{\dot\delta c}{V}\right) \quad (16)$$

$$\Delta C_{H_\delta}(S, M, e) = -\left[\frac{(1 - e)^2}{2M}\phi^i_{H_\delta}(S, M, e) + \frac{(F_5 - F_4F_{10}) + F_{12}F_{10}}{2\pi\beta}\phi^c_{H_\delta}(S, M, e)\right]\Delta\delta \quad (17)$$

$$\Delta C_{H_{\dot\delta}}(S, M, e) = -\left[\frac{(1 - e)^3}{6M}\phi^i_{H_{\dot\delta}}(S, M, e) + \frac{F_{11}(F_{12} - F_4)}{4\pi\beta}\phi^c_{H_{\dot\delta}}(S, M, e)\right]\Delta\left(\frac{\dot\delta c}{V}\right) \quad (18)$$

where the indicial response functions $\phi^c_{N_\delta}$, $\phi^c_{N_{\dot\delta}}$, $\phi^i_{N_\delta}$, $\phi^i_{N_{\dot\delta}}$, $\phi^c_{M_\delta}$, $\phi^c_{M_{\dot\delta}}$, $\phi^i_{M_\delta}$, $\phi^i_{M_{\dot\delta}}$, $\phi^c_{H_\delta}$, $\phi^c_{H_{\dot\delta}}$, $\phi^i_{H_\delta}$, and $\phi^i_{H_{\dot\delta}}$ represent the intermediate behavior of the respective indicial airloads between $S = 0$ and $S = \infty$.

During the time between the initial noncirculatory dominated loading until the final circulatory dominated loading is obtained, the flow adjustments are very complex, and involve the simultaneous creation of circulation as well as the propagation and reflection of pressure wave disturbances. Mazelsky[24] showed that the noncirculatory lift in subsonic compressible flow decays very rapidly and almost exponentially from the initial (piston theory) values. The circulatory part of the indicial response accounts for the influence of the shed wake, and it has been shown in Refs. 22 and 23 that this part of the indicial response caused by changes in airfoil angle of attack ϕ^c_α can be approximated by

$$\phi^c_\alpha(S, M) = 1 - \sum_{i=1}^{N} A_i \exp(-b_i\beta^2 S), \quad \sum A_i = 1, \quad b_i > 0 \quad (19)$$

The scaling of this function with respect to Mach number has been previously justified from experiments[22,23,25] and is simply a manifestation of the fact that the aerodynamic lag effects caused by the wake become larger with increasing Mach number. The coefficients A_i and b_i have been derived using both exact linear theory and experimental data in the frequency domain.[23] Note further, that analogous to the incompressible case, in linearized subsonic flow the circulatory lift lag also does not depend on the airfoil boundary conditions. This result was examined in some detail for the subsonic case by Mazelsky.[26,27] Therefore, for all the circulatory lift terms

$$\phi^c_{N_\alpha}(S, M) = \phi^c_{N_\alpha}(S, M, a) = \phi^c_{N_\delta}(S, M, e) = \phi^c_{N_{\dot\delta}}(S, M, e) \quad (20)$$

Since the circulatory loads from the shed wake act at the aerodynamic center (which is also the one-quarter-chord point in linear theory), the indicial moments build very rapidly to their steady-state (or quasisteady) values. It can be assumed that

$$\phi^c_{M_\delta} = \phi^c_{M_{\dot\delta}} = 1 - \exp(-b_3\beta^2 S) \quad (21)$$

Again, the time constant b_3 has been obtained based on experimental measurements in the frequency domain that have been used to relate back to the assumed form of the indicial functions.[18]

The hinge moment is dominated by the quasisteady terms, therefore, it can be assumed that

$$\phi^c_{M_\delta}(S, M) = \phi^c_{M_{\dot\delta}}(S, M) = \phi^c_{H_\delta}(S, M, e) = \phi^c_{H_{\dot\delta}}(S, M, e) \quad (22)$$

For indicial flap motion, exponential decays can also be assumed giving

$$\Delta C^i_{N_{\dot\delta}}(S, M, e) = \frac{2(1 - e)}{M}\phi^i_{N_{\dot\delta}}(S, M, e)\Delta\delta = \frac{2(1 - e)}{M}\exp\left[\frac{-S}{T'_{N_{\dot\delta}}(M, e)}\right]\Delta\delta \quad (23)$$

$$\Delta C^i_{N_{\dot\delta}}(S, M, e) = \frac{(1 - e)^2}{2M}\phi^i_{N_{\dot\delta}}(S, M, e)\Delta\left(\frac{\dot\delta c}{V}\right) = \frac{(1 - e)^2}{2M}\exp\left[\frac{-S}{T'_{N_{\dot\delta}}(M, e)}\right]\Delta\left(\frac{\dot\delta c}{V}\right) \quad (24)$$

$$\Delta C^i_{M_\delta}(S, M, e) = -\frac{(1 - e)(2 + e)}{2M}\phi^i_{M_\delta}(S, M, e)\Delta\delta = -\frac{(1 - e)(2 + e)}{2M}\exp\left[\frac{-S}{T'_{M_\delta}(M, e)}\right]\Delta\delta \quad (25)$$

$$\Delta C^i_{M_\delta}(S, M, e) = \frac{1}{12M}\left[(1+e)^3 - (12e-4) - \frac{3}{2}(1-e)^2\right] \times \phi^i_{M_\delta}(S, M, e)\Delta\left(\frac{\dot{\delta}c}{V}\right) = \frac{1}{12M}\left[(1+e)^3 - (12e-4) - \frac{3}{2}(1-e)^2\right] \times \exp\left[\frac{-S}{T'_{M_\delta}(M, e)}\right]\Delta\left(\frac{\dot{\delta}c}{V}\right) \quad (26)$$

$$\Delta C^i_{H_\delta}(S, M, e) = -\frac{(1-e)^2}{2M}\phi^i_{H_\delta}(S, M, e)\Delta\delta = -\frac{(1-e)^2}{2M}\exp\left(\frac{-S}{T'_{H_\delta}(M, e)}\right)\Delta\delta \quad (27)$$

$$\Delta C^i_{H_\delta}(S, M, e) = -\frac{(1-e)^3}{6M}\phi^i_{H_\delta}(S, M, e)\Delta\left(\frac{\dot{\delta}c}{V}\right) = -\frac{(1-e)^3}{6M}\exp\left(\frac{-S}{T'_{H_\delta}(M, e)}\right)\Delta\left(\frac{\dot{\delta}c}{V}\right) \quad (28)$$

where $T'_{N_\delta}(M)$, $T'_{M_\delta}(M)$, $T'_{H_\delta}(M)$, $T'_{N_\delta}(M)$, $T'_{M_\delta}(M)$, and $T'_{H_\delta}(M)$ are Mach number dependent time constants.

Exact Subsonic Linear Theory

The previous noncirculatory time constants can be evaluated with the aid of exact solutions for the indicial airfoil response. Lomax et al.[21] and Lomax[28] obtained theoretical results using a form of the wave-equation for the indicial responses caused from step changes in airfoil AOA and pitch rate. The mathematical calculations are somewhat complex, and solutions can be obtained only for less than one semichord length of airfoil travel, but this is still sufficient to define the initial behavior of the indicial response.

The exact solution for the chordwise pressure on an airfoil undergoing a unit step change in AOA is[21]

$$\Delta C^\alpha_p(x, \hat{t}) = \Re\left(\frac{8}{\pi(1+M)}\sqrt{\frac{\hat{t}-x}{M\hat{t}+x}} + \frac{4}{\pi M}\left\{\cos^{-1}\left[\frac{\hat{t}(1+M)-2(c-x)}{\hat{t}(1x)}\right]_{\hat{t}(1-M)} - \cos^{-1}\left[\frac{2x-\hat{t}(1-M)}{\hat{t}(1+M)}\right]\right\}\right) \quad (29)$$

Also, the exact solution for the chordwise pressure on an airfoil undergoing a unit step change in pitch rate (pitching about the leading edge) is

$$\Delta C^\alpha_p(x, \hat{t}) = \Re\left[\frac{8}{\pi Mc}\left(\sqrt{(\hat{t}-x)(M\hat{t}+x)} + \frac{M(1-M)}{3(1+M)^2}\times\sqrt{\frac{(\hat{t}-x)^3}{(M\hat{t}+x)}} - \sqrt{(c-M\hat{t}-x)(\hat{t}+x-c)} + \frac{1}{2}(M\hat{t}+x)\left\{\cos^{-1}\left[\frac{\hat{t}(1+M)-2(c-x)}{\hat{t}(1-M)}\right] - \cos^{-1}\left[\frac{2x-\hat{t}(1-M)}{\hat{t}(1+M)}\right]\right\}\right)\right] \quad (30)$$

where both equations are valid for the short period $0 \le \hat{t} \le c/(1+M)$. Note that $\Re$ refers to the real part, and in these particular equations x is measured from the airfoil leading edge. The resulting lift on the airfoil can be obtained by integration, and the result transformed to the S domain by making use of the result $S = 2M\hat{t}$ (Ref. 21).

Reverse Flow Theorems

The indicial responses from the impulsive motion of a trailing-edge flap are difficult to obtain directly but can be conveniently obtained using Eq. (29) with the aid of the reverse flow relations.[29,30] If one is only interested in the total lift and moment, it appears that this approach furnishes a rigorous way of treating the indicial flap problem exactly. The main advantage of the reverse flow theorems is that they permit a solution to the airloads for any imposed camber using only the flat-plate solution.

Consider first the indicial lift because of δ, which produces a uniform perturbation velocity over the flap. It can be shown by the reverse flow theorems that the lift in steady or indicial motion per unit angle of flap deflection is equal to the lift per unit AOA on the corresponding portion of a flat-plate airfoil moving in the reverse direction. Consider a flapped portion of one airfoil deflected at an angle δ, and the remainder of the airfoil is a flat plate with its surface parallel to the freestream. Let a second airfoil be a flat-plate airfoil at α_2, so that

$$\alpha = \begin{cases}\delta & \text{on the flap} \quad \alpha_2 = \text{const}\\ 0 & \text{elsewhere}\end{cases} \quad (31)$$

Then the reverse flow theorem gives

$$\frac{C_{N_1}(\hat{t})}{\delta} = \int_{\text{flap}}\left[\frac{\Delta C^\alpha_{P_2}\left(\frac{x_2}{c}, t\right)}{\alpha_2}\right] d\left(\frac{x_2}{c}\right) \quad (32)$$

where ΔC^α_p is given by Eq. (29) and the subscript 2 refers to the second airfoil. It was shown by Leishman[8] that in the short time interval $0 \le S \le M(1-e)/(1+M)$ the indicial lift caused by the flap deflection angle is given exactly by

$$\Delta C_{N_\delta}(S) = [2(1-e)/M]\{1 - [(1-M)S/2M(1-e)]\}\Delta\delta \quad (33)$$

From this result for the indicial flap response in subsonic flow, the time constants for the noncirculatory parts of the indicial response approximations can be obtained by equating the sum of the time derivatives of the approximate solutions to the corresponding time derivative of the exact solutions. Based on this approach, which was first outlined for the lift from flap deflection and flap rate terms in Ref. 23, the noncirculatory time constants for lift from flap deflection can be expressed as

$$T_{N_\delta}(M, e) = \left(\frac{c}{2V}\right)T'_{N_\delta} = (1-e)\left[(1-M) + 2F_{10}\beta M^2\sum_{i=1}^{2}A_i b_i\right]^{-1}\left(\frac{c}{a_s}\right) = K_{N_\delta}(M, e)T_i \quad (34)$$

Since the indicial lift response to flap deflection is now defined, it is plotted in Fig. 2. In Fig. 2a the lift is shown for small values of time where the linear theory is also valid, and Fig. 2b shows the response for extended values of time. Note

that these indicial airloads are quite different to the incompressible results, which all exhibit an infinite pulse (Dirac delta function) at $S = 0$.

A similar approach can be used to find the initial behavior of the indicial response caused from the flap rate $\dot{\delta}$, i.e., angular rotation about the hinge. The local perturbation velocity because of this motion is linear over the flap and zero at the hinge axis. By means of the reverse flow relations, it can be shown that the lift on one airfoil as a result of flap rate about the hinge is equal to the integral over the airfoil of the product of the perturbation in local AOA induced by the flap rate motion and the loading per unit AOA at the corresponding point of a second airfoil comprising a flat plate moving in the reverse direction. Therefore,

$$\frac{C_{N_1}(\hat{t})}{\frac{\dot{\delta}c}{V}} = \int_{\text{flap}} \left[\frac{\Delta C^{\alpha}_{p_2}\left(\frac{x_2}{c}, \hat{t}\right)}{\alpha_2} \right] \left[\left(\frac{1-e}{2}\right) - \frac{x_2}{c} \right] \mathrm{d}\left(\frac{x_2}{c}\right) \tag{35}$$

In the short time interval $0 \leq S \leq M(1-e)/(1+M)$, it can be shown by integration that the indicial lift because of flap rate varies as

$$\Delta C_{N_{\dot{\delta}}}(S) = \frac{1}{2M}\left[(1-e)^2 - \frac{(1-M)(1-e)S}{M} + \frac{(2-M)S^2}{2M}\right] \Delta\left(\frac{\dot{\delta}c}{V}\right) \tag{36}$$

By following the same procedure as for the lift where the gradients are matched at $S = 0$, then the time constant can be written as

$$T_{N_{\dot{\delta}}}(M, e) = \left(\frac{c}{2V}\right) T'_{N_{\dot{\delta}}} = \frac{(1-e)^2}{2}\left[(1-M)(1-e) + F_{11}\beta M^2 \sum_{i=1}^{2} A_i b_i\right]^{-1}\left(\frac{c}{a_s}\right) = K_{N_{\dot{\delta}}}(M, e)T_i \tag{37}$$

The results for the indicial lift from the flap rate are plotted in Fig. 3 for short and extended values of time.

Another set of reverse flow theorems can be used to find the pitching moment on the airfoil from the flap motion. It can be shown that the pitching moment on one airfoil because of flap deflection is equal to the integral over the airfoil of the product of the local AOA induced by the flap deflection motion and the loading per unit pitch rate at the corresponding point of a second airfoil comprising of a flat plate moving in the reverse direction. Therefore,

$$\frac{C_{M_1}(\hat{t})}{\delta} = \int_{\text{flap}} \left[\frac{\Delta C^{\alpha}_{p_2}\left(\frac{x_2}{c}, \hat{t}\right)}{\frac{\dot{\alpha}_2 c}{V}} \right] \mathrm{d}\left(\frac{x_2}{c}\right) - \frac{3}{4}\int_{\text{flap}} \left[\frac{\Delta C^{\alpha}_{p_2}\left(\frac{x_2}{c}, \hat{t}\right)}{\alpha} \right] \mathrm{d}\left(\frac{x_2}{c}\right) \tag{38}$$

where the second term on the right-hand side (RHS) of the previous equation is from the difference in the axis locations of the first and the second airfoils. It can be shown by integration that in the short time interval $0 \leq S \leq M(1-e)/(1+M)$ the indicial pitching moment about the one-quarter-chord from the flap deflection angle is given by

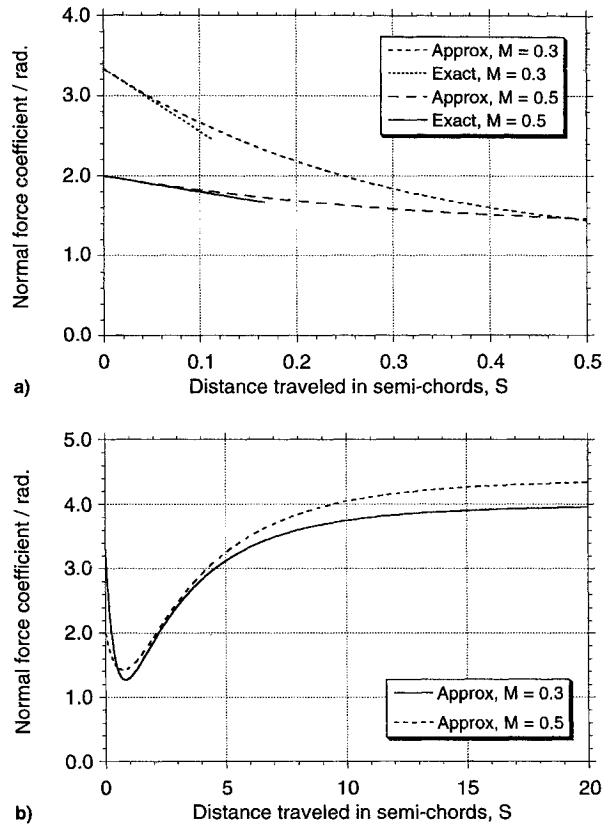

Fig. 2 Indicial lift because of flap displacement at $M = 0.3$ and 0.5: a) short values of time and b) for an extended time.

$$\Delta C_{M_{\dot{\delta}}}(S) = -(1/2M)\{(1-e)(2+e) - [3(1-M)/2M]S - [(2-M)/2M]S^2\}\Delta\dot{\delta} \tag{39}$$

In this case, the noncirculatory time constant is

$$T_{M_{\dot{\delta}}}(M, e) = (c/V)T'_{M_{\dot{\delta}}} = (1-e)(2+e)[3(1-M) + 2(F_4 + F_{10})\beta M^2 b_3]^{-1}(c/a_s) = K_{M_{\dot{\delta}}}(M, e)T_i \tag{40}$$

and the result for the indicial moment response from the displacement of the flap is plotted in Fig. 4.

The reverse flow theorems show that the pitching moment on one airfoil because of flap rate about the hinge is equal to the integral over the airfoil of the product of the perturbation in local AOA induced by the flap rate motion and the loading per unit pitch rate at the corresponding point of the second airfoil comprising a flat plate moving in the reverse direction. Therefore,

$$\frac{C_{M_1}(\hat{t})}{\frac{\dot{\delta}c}{V}} = \int_{\text{flap}} \left[\frac{(1-e)}{2} - \frac{x_2}{c}\right] \left[\frac{\Delta C^{\alpha}_{p_2}\left(\frac{x_2}{c}, \hat{t}\right)}{\frac{\dot{\alpha}_2 c}{V}} \right] \mathrm{d}\left(\frac{x_2}{c}\right) - \frac{3}{4}\int_{\text{flap}} \left[\frac{(1-e)}{2} - \frac{x_2}{c}\right] \left[\frac{\Delta C^{\alpha}_{p_2}\left(\frac{x_2}{c}, \hat{t}\right)}{\alpha} \right] \mathrm{d}\left(\frac{x_2}{c}\right) \tag{41}$$

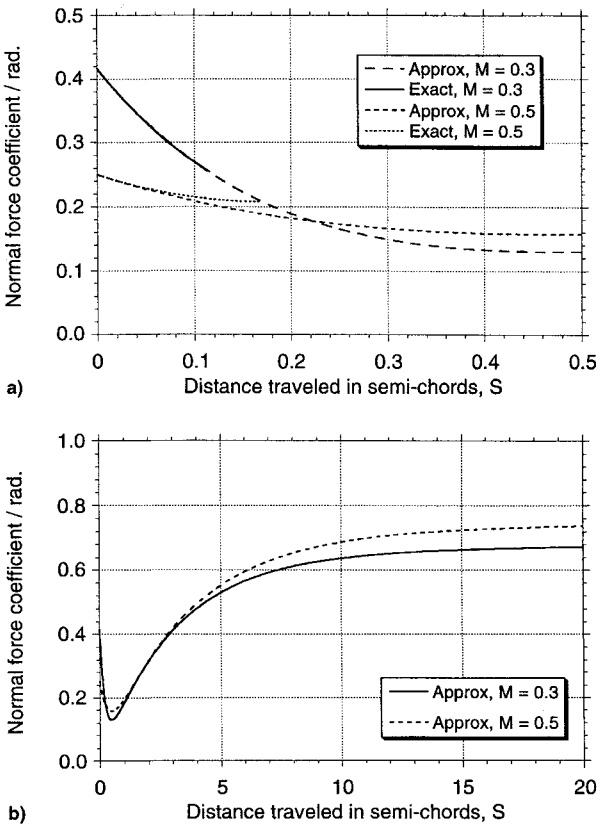

Fig. 3 Indicial lift because of flap rate at M = 0.3 and 0.5: a) short values of time and b) for an extended time.

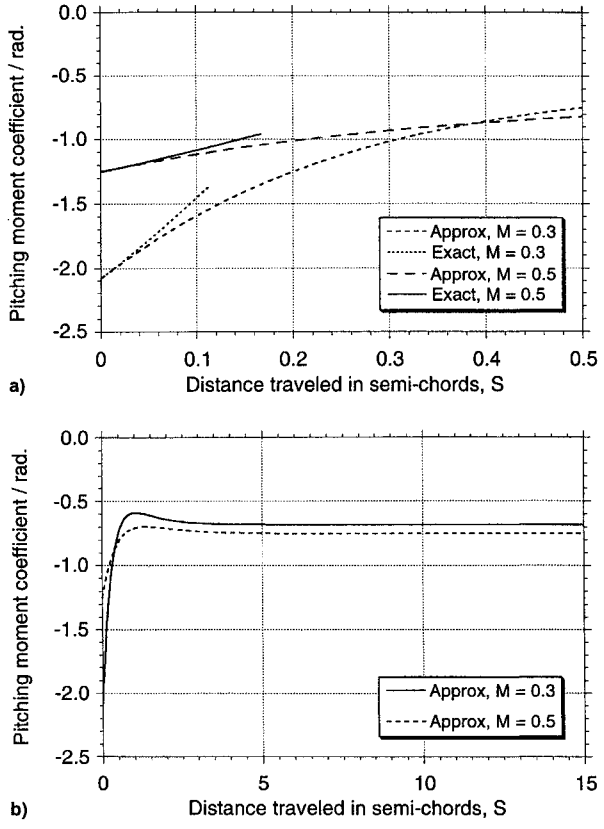

Fig. 4 Indicial airfoil moment because of flap displacement at M = 0.3 and 0.5: a) short values of time and b) for an extended time.

where the second term on the RHS of the previous equation is from the difference in the axis locations of the first and the second airfoils. It can be shown by integration that in the short time interval $0 \leq S \leq M(1 - e)/(1 + M)$ the indicial pitching moment about the one-quarter-chord from the flap rate is given exactly by

$$\Delta C_{M_{\dot\delta}}(S) = -\frac{1}{12M}\left\{(1+e)^3 - (12e-4) - \frac{3(1-e)^2}{2} - \left[\frac{9(1-M)(1-e)}{2M}\right]S + \left[\frac{3(2-M)(1+2e)}{4M}\right]S^2 + \left[\frac{(1-M)^3+4M}{4M^3}\right]S^3\right\}\dot\delta \tag{42}$$

The time constant in this case is given by

$$T_{M_{\dot\delta}}(M,e) = (c/2V)T'_{M_{\dot\delta}} = \{(1+e)^3 - (12e-4) - [3(1-e)^2/2]\}[9(1-M)(1-e) + 6[F_1 - F_8 - (e+0.5)F_4 + (F_{11}/2)]\beta M^2 b_3\}^{-1}(c/a_s) = K_{M_{\dot\delta}}(M,e)T_i \tag{43}$$

with the indicial moment response from the angular rotation rate of the flap being plotted in Fig. 5.

Note that in the previous representation, no matter what the actual values selected for the circulatory coefficients A_i, b_i, etc., the noncirculatory time constants always give the correct initial behavior of the total indicial response as given by the exact linear theory.

Recall that the reverse flow theorems apply to only total forces and moments. Therefore, the exact values for the time–history of the hinge moment (which involves partial integration of the pressure distribution), cannot be found by using the reverse flow theorems in the same manner. However, an alternate expression, namely the airfoil moment about the hinge, which is simply a translation of the airfoil moment from the one-quarter-chord to the hinge, can be calculated. This includes the entire loading on the airfoil, whereas the hinge moment includes only the loading on the flap. At $S = 0$ the entire loading on the airfoil is concentrated only on the flap, and so the airfoil moment about the hinge is equal to the hinge moment. It is, therefore, justified in assuming that the hinge moment and the airfoil moment about the hinge will be approximately the same for small values of times after the perturbation is applied. This assumption leads to

$$T_{H_{\dot\delta}}(M,e) = 2\pi(1-e)^2[4\pi(1-M)(1-e) + 4(F_5 - F_4F_{10} + F_{12}F_{10})\beta M^2 b_3]^{-1}(c/a_s) = (c/2V)T'_{H_{\dot\delta}} = K_{H_{\dot\delta}}(M,e)T_i \tag{44}$$

$$T_{H_{\ddot\delta}}(M,e) = 2\pi(1-e)^3[6\pi(1-M)(1-e)^2 + 6F_{11}(F_{12} - F_4)\beta M^2 b_3]^{-1}(c/a_s) = (c/2V)T'_{H_{\ddot\delta}} = K_{H_{\ddot\delta}}(M,e)T_i \tag{45}$$

Results for the indicial flap hinge moment because of impulsive trailing-edge flap deflection and rate are shown in Fig. 6 for M = 0.3 and 0.5. Note that compared to the other indicial responses, the hinge moments attain their steady-state values much more quickly, and suggests that for most low- or medium-frequency applications the hinge moment may be adequately modeled by means of quasisteady theory.

Arbitrary Flap Motion

The indicial flap lift and moment responses obtained previously are solutions to specific forms of input motions, which are only mathematically realizable. For any practical arbitrary

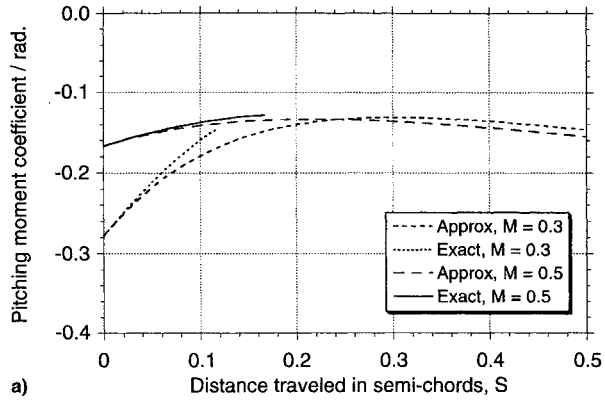

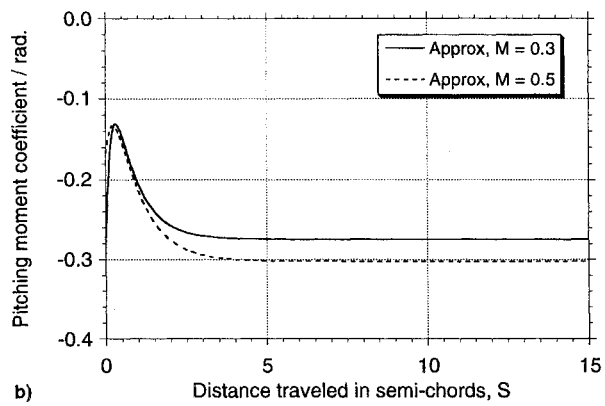

Fig. 5 Indicial airfoil moment because of flap rate at M = 0.3 and 0.5: a) short values of time and b) for an extended time.

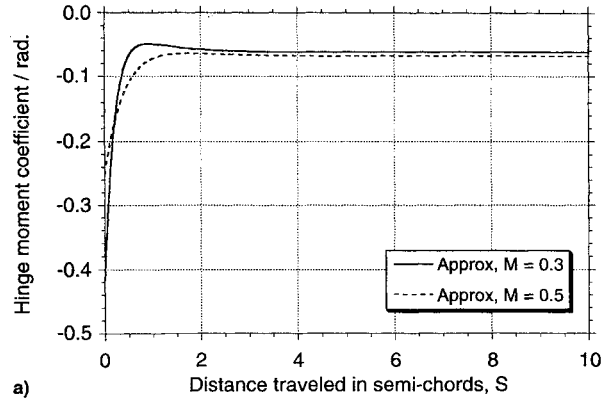

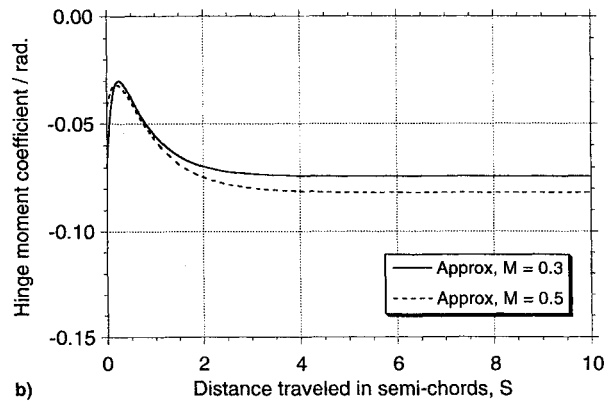

Fig. 6 Indicial hinge moment because of a) flap displacement and b) flap rate at M = 0.3 and 0.5.

flap motion, it is necessary to use Duhamel superposition to calculate the unsteady aerodynamic forces and moments using the previously obtained indicial responses. As discussed previously, there are two commonly used approaches, namely, the state–space formulation and the recursive formulation. In the present article, the state–space form will be described, although the corresponding recursive formulation is given in Ref. 19.

Consider the lift response because of arbitrary flap deflection in subsonic flow. Since the circulatory part of the indicial response does not depend on the mode of forcing, the flap deflection angle and the pitch rate about the hinge can be combined into a single term, δ_{qs}, where

$$\delta_{qs} = [(F_{10}\delta/\pi) + (bF_{11}\dot{\delta}/2\pi V)] \tag{46}$$

The state–space form for the circulatory part of the unsteady lift because of the flap motion can then be written as

$$\begin{bmatrix} \dot{z}_1(t) \\ \dot{z}_2(t) \end{bmatrix} = \begin{bmatrix} 0 & 1 \\ -b_1 b_2 \left(\frac{2V}{c}\right)^2 \beta^4 & -(b_1 + b_2)\left(\frac{2V}{c}\right)\beta^2 \end{bmatrix} \times \begin{bmatrix} z_1(t) \\ z_2(t) \end{bmatrix} + \begin{bmatrix} 0 \\ 1 \end{bmatrix} \delta_{qs}(t) \tag{47}$$

with the output equation

$$C_N^c(t) = \frac{2\pi}{\beta}\begin{bmatrix} (b_1 b_2)\left(\frac{2V}{c}\right)^2 \beta^4 & (A_1 b_1 + A_2 b_2)\left(\frac{2V}{c}\right)\beta^2 \end{bmatrix} \times \begin{bmatrix} z_1(t) \\ z_2(t) \end{bmatrix} \tag{48}$$

Note that the coefficients A_1, b_1, etc., as given by Eq. (19), are defined in Refs. 20 and 23.

It was noted earlier that the circulatory moments approach their steady-state values in a very short period, and these can be written in state–space form as

$$\dot{z}_3(t) = -(2V/c)b_3\beta^2 z_3(t) + \delta_{qs_M}(t) \tag{49}$$

with the output equation

$$C_M^c(t) = (\pi/\beta)b_3\beta^2(2V/c)z_3(t) \tag{50}$$

In this case $\delta_{qs_M}(t)$ is given by

$$\delta_{qs_M}(t) = -\left(\frac{F_4 + F_{10}}{2\pi\beta}\right)\delta - \left[\frac{2F_1 - 2F_8 - (2e+1)F_4 + F_{11}}{8\pi\beta}\right]\left(\frac{\dot{\delta}c}{V}\right) \tag{51}$$

A similar approach for the hinge moment results in

$$\dot{z}_4(t) = -(2V/c)b_3\beta^2 z_4(t) + \delta_{qs_H}(t) \tag{52}$$

with the output equation

$$C_H^c(t) = (\pi/\beta)b_3\beta^2(2V/c)z_4(t) \tag{53}$$

and where in this case

$$\delta_{qs_H}(t) = -\left(\frac{F_5 - F_4F_{10} + F_{12}F_{10}}{2\pi\beta}\right)\delta - \left[\frac{F_{11}(F_{12} - 2F_4)}{4\pi\beta}\right]\left(\frac{\dot{\delta}c}{V}\right) \tag{54}$$

Recall that the noncirculatory lift and moment components also have a time–history effect in subsonic compressible flow.

Also, their effects cannot be combined and must be considered separately since their respective loadings are governed by different time-constants.

The noncirculatory parts of the unsteady lift, airfoil moment, and hinge moment from arbitrary flap deflection $\delta(t)$ can be written as

$$\dot{z}_5(t) = \delta(t) - \frac{1}{K_{N_\delta} T_i} z_5(t), \quad C^i_{N_\delta}(t) = \Delta C_{N_\delta}(S=0, M)\dot{z}_5(t) \tag{55}$$

$$\dot{z}_6(t) = \delta(t) - \frac{1}{K_{M_\delta} T_i} z_6(t), \quad C^i_{M_\delta}(t) = \Delta C_{M_\delta}(S=0, M)\dot{z}_6(t) \tag{56}$$

$$\dot{z}_7(t) = \delta(t) - \frac{1}{K_{H_\delta} T_i} z_7(t), \quad C^i_{H_\delta}(t) = \Delta C_{H_\delta}(S=0, M)\dot{z}_7(t) \tag{57}$$

where $\Delta C_{N_\delta}(S=0, M)$, $\Delta C_{M_\delta}(S=0, M)$, and $\Delta C_{H_\delta}(S=0, M)$ are the initial values of the respective indicial responses as given previously.

Similarly, the noncirculatory lift, airfoil moment, and hinge moment because of arbitrary flap rate about the hinge $\dot{\delta}(t)$ can be written as

$$\dot{z}_8(t) = \frac{\dot{\delta}(t)c}{V} - \frac{1}{K_{N_{\dot\delta}} T_i} z_8(t), \quad C^i_{N_{\dot\delta}}(t) = \Delta C_{N_{\dot\delta}}(S=0, M)\dot{z}_8(t) \tag{58}$$

$$\dot{z}_9(t) = \frac{\dot{\delta}(t)c}{V} - \frac{1}{K_{M_{\dot\delta}} T_i} z_9(t), \quad C^i_{M_{\dot\delta}}(t) = \Delta C_{M_{\dot\delta}}(S=0, M)\dot{z}_9(t) \tag{59}$$

$$\dot{z}_{10}(t) = \frac{\dot{\delta}(t)c}{V} - \frac{1}{K_{H_{\dot\delta}} T_i} z_{10}(t), \quad C^i_{H_{\dot\delta}}(t) = \Delta C_{H_{\dot\delta}}(S=0, M)\dot{z}_{10}(t) \tag{60}$$

Flap Effectiveness

The preceding analysis applies to flaps that are 100% efficient; that is, there is no loss of flap effectiveness in the creation of aerodynamic loads because of viscous effects. In practice, a trailing-edge flap may operate in a relatively thick turbulent boundary layer. Also, the presence of the flap hinge produces a locally adverse pressure gradient, and tends to thicken the boundary layer with the application of flap deflection. This will alter the effective flap camber, and reduce the flap effectiveness for a given flap deflection angle.[31] In addition, the influence of the flap hinge geometry, and the possibility of a gap at the hinge, leads to additional viscous effects that may adversely alter the relationship between the flap deflection angle and the aerodynamic forces and moments.[32]

To a first order, it is possible to account for such effects by the application of flap effectiveness coefficients. Since it is likely that the lift, moment, and hinge moment will be influenced by different amounts by the application of a flap, each component of the loading must be considered separately. Flap effectiveness coefficients can be derived most accurately by empirical means, but only on the basis of steady flow considerations; that is, based only on circulatory effects and with regard to measurements of the static aerodynamic coefficients with flap angle and gap size. Therefore, it is possible to write the actual aerodynamic forces and moments as the linear theory values multiplied by constant terms, ε_N, ε_M, and ε_H, where these apply to the lift force, moment, and hinge moment respectively. In practice, these values may range in value from close to unity to about 0.5, and may be a function of Mach number. As shown later, in the present work the values for these coefficients have been estimated from the quasisteady data of Ref. 33.

Unsteady Drag

The unsteady drag is of considerable importance in rotorcraft work. The calculation of the unsteady drag in subsonic compressible flow is somewhat involved, yet can be achieved following a procedure first outlined for the incompressible case by Garrick.[34] When resolved in a space-fixed coordinate system, the pressure drag can be written as

$$C_D = (C_N\alpha + C_F\delta) - C_S \tag{61}$$

where C_S is the leading-edge suction force. For the subsonic case, this is

$$C_S = (2\pi/\beta)A_0^2 \tag{62}$$

where C_F is the force coefficient on the control surface, and A_0 is the leading term in the pressure distribution as given by quasisteady, thin airfoil theory, i.e.,

$$A_0 = \alpha_{\text{eff}} + \left(\frac{\dot\alpha c}{2V}\right)_{\text{eff}} + \cos^{-1}e\,\frac{\delta_{\text{eff}}}{\pi} + \left(\frac{\dot\delta c}{V}\right)_{\text{eff}}\left(\frac{\sqrt{1-e^2} - e\cos^{-1}e}{2\pi}\right) \tag{63}$$

The effective AOA pitch rate, flap deflection, and flap rate are given by

$$\alpha_{\text{eff}} = C^c_{N_\alpha}\beta/2\pi \quad (\dot\alpha c/2V)_{\text{eff}} = C^c_{N_{\dot\alpha}}\beta/2\pi \tag{64}$$

$$\delta_{\text{eff}} = C^c_{N_\delta}\beta/2F_{10} \quad (\dot\delta c/V)_{\text{eff}} = 2C^c_{N_{\dot\delta}}\beta/F_{11} \tag{65}$$

where $C^c_{N_\alpha}$, $C^c_{N_{\dot\alpha}}$, $C^c_{N_\delta}$, and $C^c_{N_{\dot\delta}}$ are the circulatory components of the unsteady lift from the AOA, pitch rate, flap deflection, and flap rate, respectively.

Again, the effects of viscosity enter into the problem, even at low AOAs, since the effects of finite airfoil thickness tend to reduce the maximum attainable leading-edge suction. This can be accounted for by the application of a leading-edge suction recovery factor η, which is multiplied with the theoretical value of C_S (Ref. 35). The net effect is an increase in quasisteady pressure drag proportional to δ^2 at any given AOA.

The flap force coefficient can be split into flap force coefficients because of individual modes of forcing, viz., α, $\dot\alpha$, δ, and $\dot\delta$. Furthermore, these coefficients can be resolved into the circulatory and noncirculatory components. Their initial and final values are

$$\Delta C_{F_\alpha}(S=0, M) = \frac{2(1-e)}{M}\Delta\alpha \tag{66}$$

$$\Delta C_{F_{\dot\alpha}}(S=0, M) = \frac{(1-e)(2+e)}{2M}\Delta\left(\frac{\dot\alpha c}{V}\right) \tag{67}$$

$$\Delta C_{F_\delta}(S=0, M) = \frac{2(1-e)}{M}\Delta\delta \tag{68}$$

$$\Delta C_{F_{\dot\delta}}(S=0, M) = \frac{(1-e)^2}{2M}\Delta\left(\frac{\dot\delta c}{V}\right) \tag{69}$$

$$\Delta C_{F_\alpha}(S=\infty, M) = \frac{2F_{20}}{\beta}\Delta\alpha \tag{70}$$

$$\Delta C_{F_{\dot\alpha}}(S=\infty, M) = \frac{2F_{20}}{\beta}\Delta\left(\frac{\dot\alpha c}{2V}\right) \tag{71}$$

$$\Delta C_{F_\delta}(S=\infty, M) = \frac{2F_{20}F_{10} + 2(1-e^2)}{\pi\beta}\Delta\delta \tag{72}$$

$$\Delta C_{F_\delta}(S=\infty, M) = \frac{F_{20}F_{11} + \sqrt{(1-e^2)}(1-e)}{2\pi\beta}\Delta\left(\frac{\dot{\delta}c}{V}\right) \quad (73)$$

The evaluation of the noncirculatory time constants for the flap force coefficients require the exact knowledge of the total response for small values of time. The flap force coefficients from the indicial airfoil motion can be obtained directly by the integration of Eqs. (29) and (30) over the flap region. The resulting time constants can be written as

$$T_{F_\alpha}(M, e) = \left(\frac{c}{2V}\right) T'_{F_\alpha} = (1-e) \times \left[(1-M) + 2F_{20}\beta M^2 \sum_{i=1}^{2} A_i b_i\right]^{-1} \left(\frac{c}{a_s}\right) = K_{F_\delta}(M, e)T_i \quad (74)$$

$$T_{F_{\dot\alpha}}(M, e) = \left(\frac{c}{2V}\right) T'_{F_{\dot\alpha}} = \frac{(1-e)(2+e)}{2} \times \left[2(1-M) + 4F_{20}\beta M^2 \sum_{i=1}^{2} A_i b_i\right]^{-1} \left(\frac{c}{a_s}\right) = K_{F_{\dot\alpha}}(M, e)T_i \quad (75)$$

To evaluate the time constants because of the flap motion, the exact expression for the flap force coefficient cannot be obtained using the reverse flow theorems. As an alternative, the exact expression for the normal force coefficient can be used. This can be justified since the initial values of the indicial response of the flap force and the normal force are equal for flap motion. The time constants can be written as

$$T_{F_\delta}(M, e) = (1-e)\pi\left\{\pi(1-M) + 2[F_{20}F_{10} + (1-e^2)]\beta M^2 \sum_{i=1}^{2} A_i b_i\right\}^{-1} \left(\frac{c}{a_s}\right) = \left(\frac{c}{2V}\right) T'_{F_\delta} = K_{F_\delta}(M, e)T_i \quad (76)$$

$$T_{F_{\dot\delta}}(M, e) = \frac{(1-e)^2\pi}{2}\left\{\pi(1-M)(1-e) + [F_{11}F_{20} + \sqrt{(1-e^2)}(1-e)]\beta M^2 \sum_{i=1}^{2} A_i b_i\right\}^{-1} \left(\frac{c}{a_s}\right) = \left(\frac{c}{2V}\right) T'_{F_{\dot\delta}} = K_{F_{\dot\delta}}(M, e)T_i \quad (77)$$

For an arbitrary combination of airfoil and flap motions, the flap force can be calculated as before. Once the flap force coefficient is known, the drag can be computed using Eq. (61). Further details are given in Ref. 19.

Results and Discussion

Experiments on airfoils with time-dependent flap motions are relatively rare. However, Drescher[13] has measured the time-dependent lift on an airfoil during impulsive motion of a trailing-edge flap. The unsteady surface pressures on an airfoil were measured during a ramp ($\dot\delta \approx$ const) motion of the flap, and were also compared to incompressible unsteady thin airfoil theory. Some of Drescher's results are reproduced in Ref. 36.

The present theory has been compared with Drescher's measurements, and a selection of results are shown in Fig. 7 with the remainder of the results in Ref. 19. In the test conditions shown here the airfoil was maintained at a constant AOA of $\alpha = -5$ deg (to avoid flow separation), while the flap was displaced from 0 to 15 deg at a nominally constant rate. The two cases shown in Fig. 7 are for $\dot\delta c/V = 0.048$ and $\dot\delta c/V = 0.194$. The flap motion time–history was digitized from Ref. 13 and used as an input to the aerodynamic model.

Note that immediately after the flap motion starts, the noncirculatory loads dominate the loading, and the normal force decays quickly after the flap motion has stopped. As explained previously, this is because the noncirculatory terms decay extremely rapidly after the input is terminated. On the other hand, at these early times the circulatory loadings have not yet had sufficient time to buildup. The combination of the decay of the noncirculatory loading and the slow buildup of the circulatory loading lead to a local minimum in the total normal force just after the cessation of the flap motion. After this time, the circulatory loads dominate and the normal force finally reaches its asymptotic value after about 20 semichords of airfoil travel. The agreement of the theory with the experimental data is quite good, and lends considerable support to the validity of the model.

Experimental results for oscillating flap motion on a NACA 64A006 airfoil were measured by Tijdeman and Schippers[33] and Zwaan.[37] The main emphasis in this work was for the high subcritical and transonic flow cases, but some of the results are given for shock-free flow and weak transonic conditions. Under these conditions nonlinear effects are relatively mild, and the results can be expected to provide a useful basis for comparison with the present theory. Some additional results for an oscillating flap on a NLR 7301 airfoil are given by Zwaan,[38] although these data are more limited in scope.

From the indicial response equations given previously, the airloads to a particular harmonic motion of the flap can be derived in closed form by means of Laplace transforms. While the algebraic manipulations are somewhat lengthy, explicit expressions can be readily obtained for the lift, moment, and hinge moment on the airfoil for a prescribed harmonic forcing

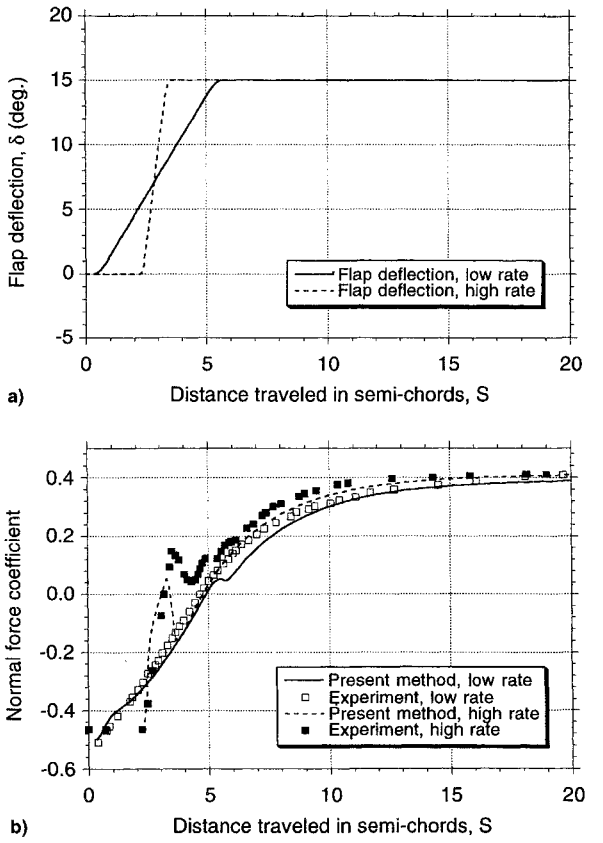

Fig. 7 Comparison of theory with Drescher's experiment for impulsive flap deflection. Low rate, $\dot\delta c/V = 0.048$ and high rate, $\dot\delta c/V = 0.194$.

as a function of flap frequency and Mach number.[19] This also provides a check of the aerodynamic approximations independently of any numerical integration of the state equations.

Typical computed results for an oscillatory flap motion are shown in Figs. 8 and 9. The flap was 25% of the airfoil chord, i.e., $e = 0.5$, and the amplitude of the oscillation at each test point was about 2.5 deg with a mean airfoil AOA of 0 deg. The results in Figs. 8 and 9 are presented as real (in-phase) and imaginary (in-quadrature) parts, which are normalized by the flap amplitude in the same manner used in Ref. 33, for a given physical frequency and over a range of Mach numbers. Note, therefore, that in these plots the reduced frequency varies as a function of Mach number. Also, the maximum reduced frequency at $M = 0.7$ is about 0.3, which is high enough so that the noncirculatory terms become significant. Unfortunately, the same range of measurements are not available at all four oscillation frequencies ($f = 0$, 30, 90, and 120 Hz), however, the range of test conditions are still wide enough to cover the range of Mach numbers and reduced frequencies typical of those found on rotorcraft.

For steady conditions ($f = 0$), the lift, moment, and hinge moment all showed excellent agreement with the measurements. Here, there is no unsteady effect, and so the imaginary parts of the response are identically zero. A flap lift effectiveness of 68% was found to provide good agreement with the real part of the lift response at $f = 0$, and this value was assumed constant over the entire Mach number and frequency range. As shown in Fig. 8 with increasing frequency there is a decrease in the magnitude of the real part of the lift response over the whole Mach number range, with a corresponding increase in the magnitude of the imaginary part. Generally, this corresponds to an increase in the phase lag of the lift with respect to the flap forcing. The agreement of the theory with the test data is seen to be good over most of the conditions.

Figure 9 shows that the real part of the airfoil (one-quarter-chord) moment from the flap motion deviates little from the quasisteady result. This is expected, since an examination of the relevant equations when written in the frequency domain show that the real part is dominated by the circulatory part of the moment, which is almost quasisteady in nature. A flap effectiveness of 96% was found to be applicable for this component of the loading, which again, was held constant over the entire Mach number and frequency range. The noncirculatory part of the moment, however, while relatively small in magnitude, significantly influences the phase of the response. At low Mach numbers, the moment leads the flap forcing, yet this slowly changes to a phase lead as the Mach number increases through about 0.8. This behavior is also shown in the experimental data, and the theory compares quite favorably with the data for all of the various conditions. The incompressible theory will not predict this behavior because a phase lead is always obtained because of the apparent mass terms. These differences between the incompressible and subsonic theory arise because in reality pressure perturbations propagate through the flow at the local speed of sound. At higher flap frequencies, even when the freestream Mach number is low, the disturbances do not propagate quickly enough relative to the flap motion for the flow to be considered incompressible. Figure 9 shows that there is some deviation between the theory and test data at the highest Mach numbers and flap frequencies, but bearing in mind that some degree of nonlinear behavior would be expected here, the agreement obtained is still good. For maximum fidelity, it might be possible to correct the theory by using a mean aerodynamic center location as a function of Mach number; however, this is outside the scope of the present work.

The flap hinge moment is probably the most difficult quantity to predict accurately since it is sensitive to viscous effects. The flap operates in the turbulent boundary layer near the trailing-edge of the airfoil and this boundary layer is strongly influenced by the local geometry and pressure gradients produced near the flap hinge. For the present work a hinge moment effectiveness of 68% was inferred from the measured quasisteady ($f = 0$) aerodynamic data. As shown in Fig. 10

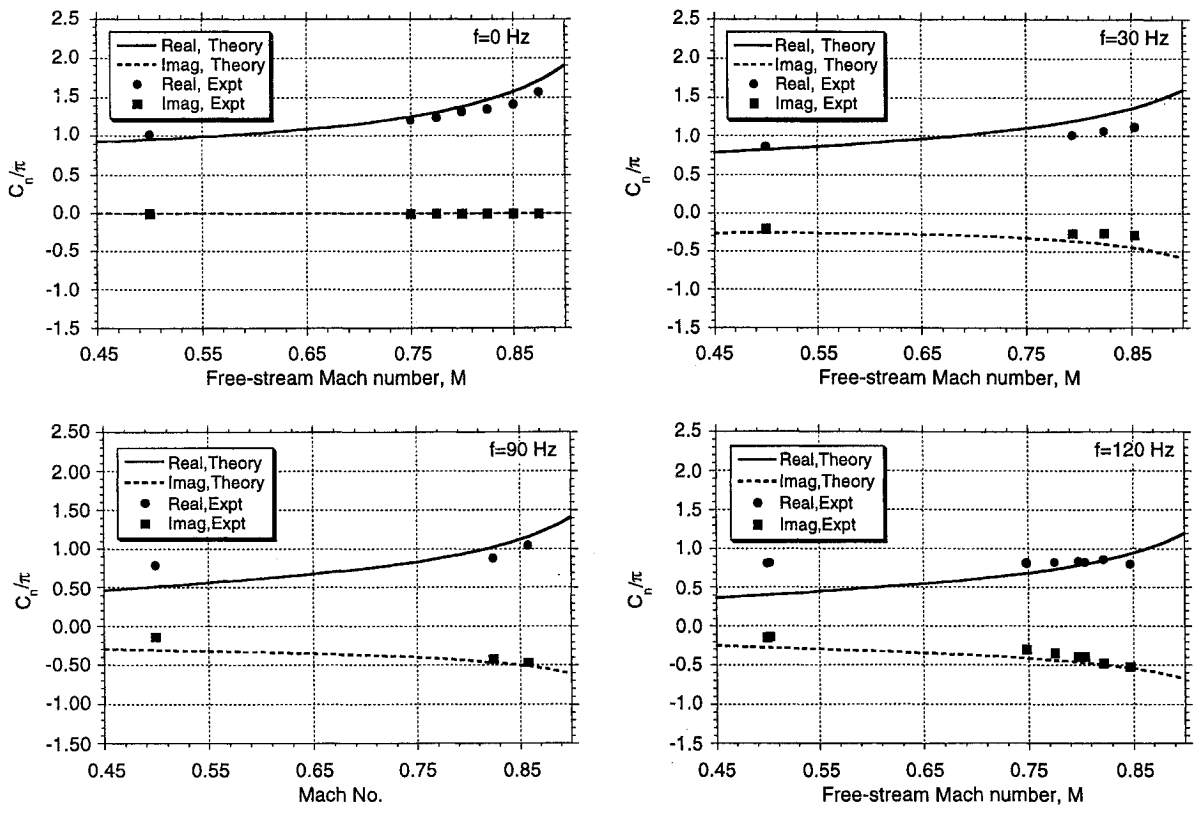

Fig. 8 Comparison of theory with experiment for the unsteady lift vs Mach number for flap oscillation frequencies of 0, 30, 90, and 120 Hz.

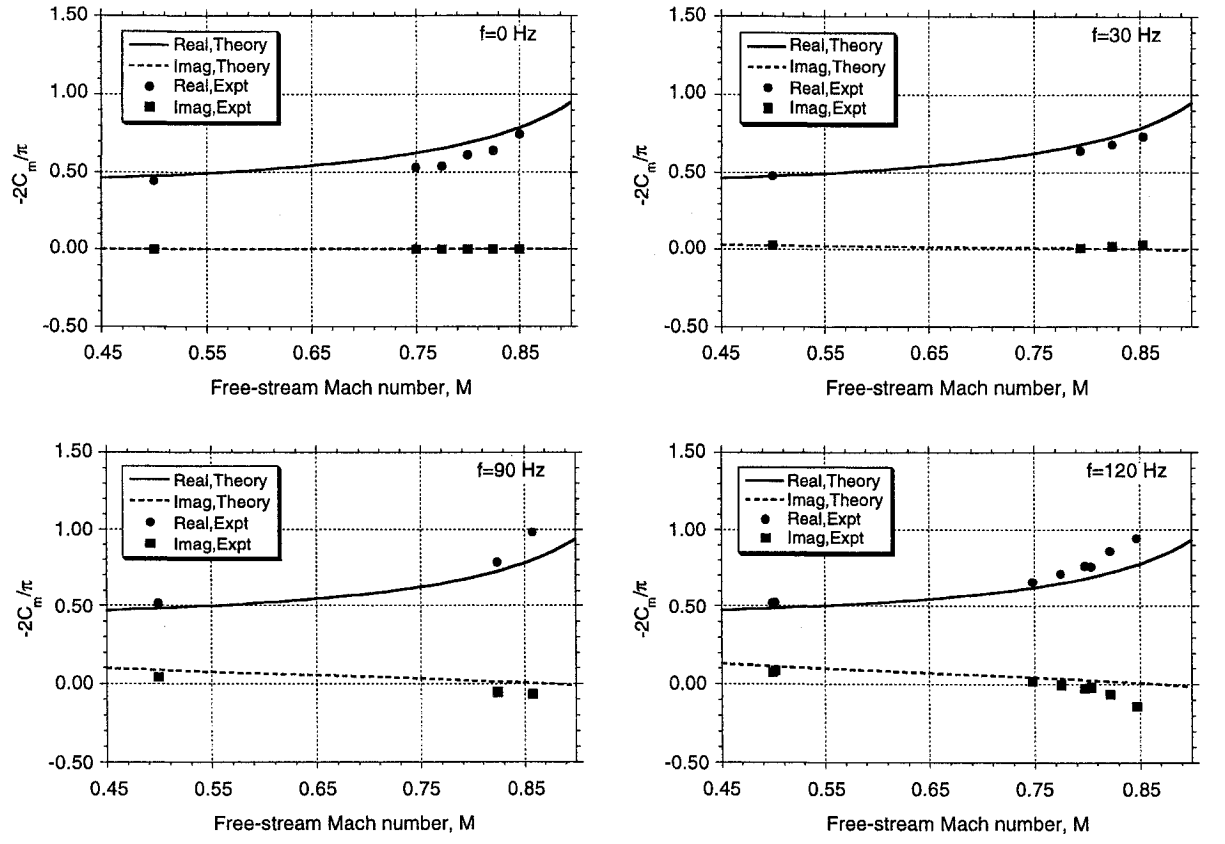

Fig. 9 Comparison of theory with experiment for the unsteady airfoil moment vs Mach number for flap oscillation frequencies of 0, 30, 90, and 120 Hz.

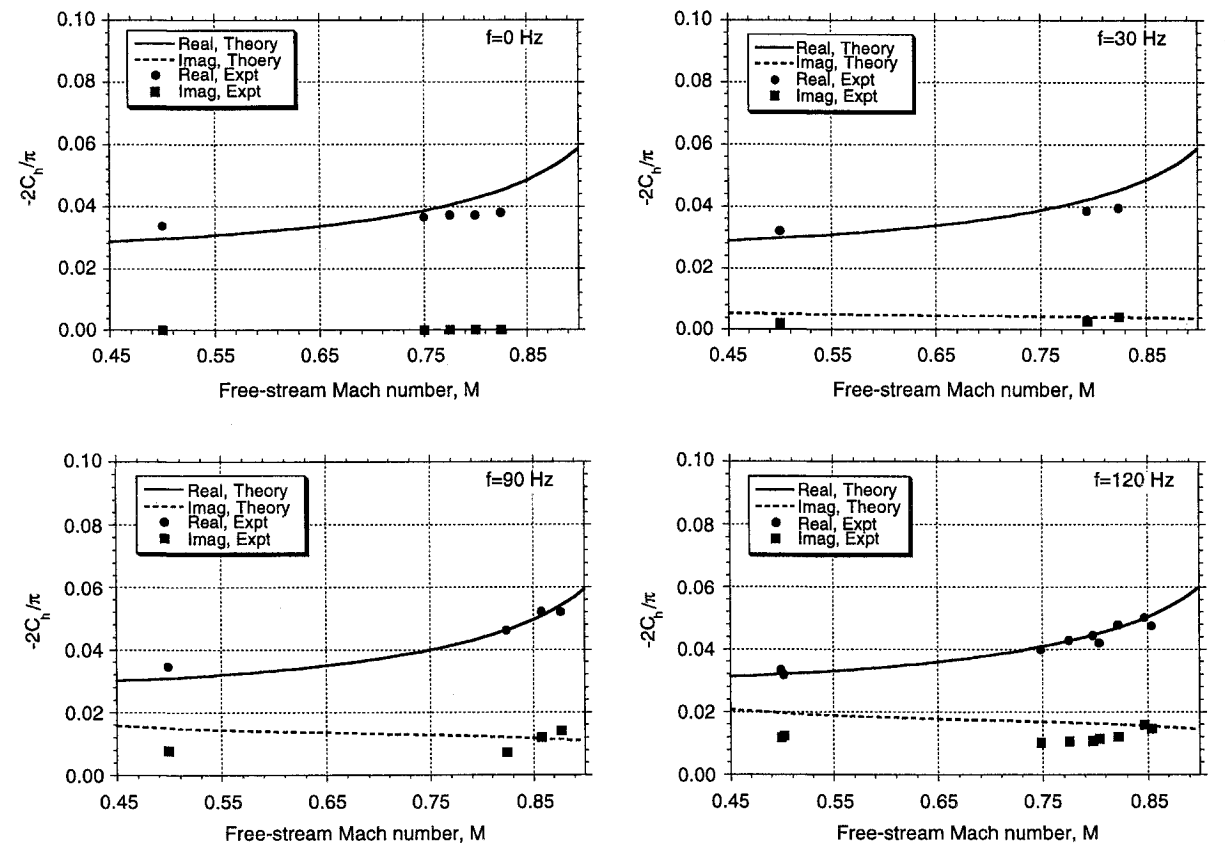

Fig. 10 Comparison of theory with experiment for the unsteady hinge moment vs Mach number for flap oscillation frequencies of 0, 30, 90, and 120 Hz.

the real part of the hinge moment is only weakly affected by flap frequency since, like the airfoil moment, the real part of the flap hinge moment is dominated by the circulatory loads. However, the imaginary part of the hinge moment is considerably more sensitive, this being dominated by the noncirculatory terms and considerably more so than the airfoil (one-quarter-chord) pitching moment discussed previously. Note that the effect of increasing flap frequency is to produce an increasing phase lead over the entire Mach number range. The agreement of the theory with the test data over the entire range is excellent, even in the transonic range where nonlinear effects might be expected. Overall, the results shown in Figs. 8 and 9 tend to confirm aerodynamic linearity over the test conditions made available in Ref. 33. However, further measurements at higher flap deflection amplitudes and/or mean AOAs would be required to fully explore the limitations of the unsteady linear theory for general use.

Another, and perhaps more intuitive, way of looking at these data is in the time domain. This is done by integrating the state equations (given previously) with respect to time using a standard ordinary differential equation solver. Typical results are shown in Fig. 11 for two conditions, one at the lowest Mach number of 0.5, and the other for $M = 0.748$. Also included in these plots are the incompressible[11] results, with the steady-state lift–curve–slope corrected by the Glauert factor $1/\beta$. When plotted vs flap displacement angle, the lift exhibits a characteristic elliptical loop, which is similar to that obtained on an airfoil oscillating in AOA. Note that in Fig. 11 the lift loops are circumvented in a counterclockwise direction, corresponding to a phase lag. At higher flap frequencies, the lift can develop a phase lead as the noncirculatory terms begin to dominate the solution. However, as shown previously, the effects of increasing freestream Mach number also tend to increase the circulatory lag, which means that the lift mostly lags the flap forcing over the range of conditions typically encountered in practice. This is shown for the $M = 0.748$ case in Fig. 11, where despite the higher reduced frequency, the phase lag is considerably greater than for the $M = 0.5$ case. Note that the incompressible results do not correlate as well with the experimental results. The incompressible theory does not predict the phasing correctly, and this is more pronounced at the higher Mach number, which is more typical of the rotor environment.

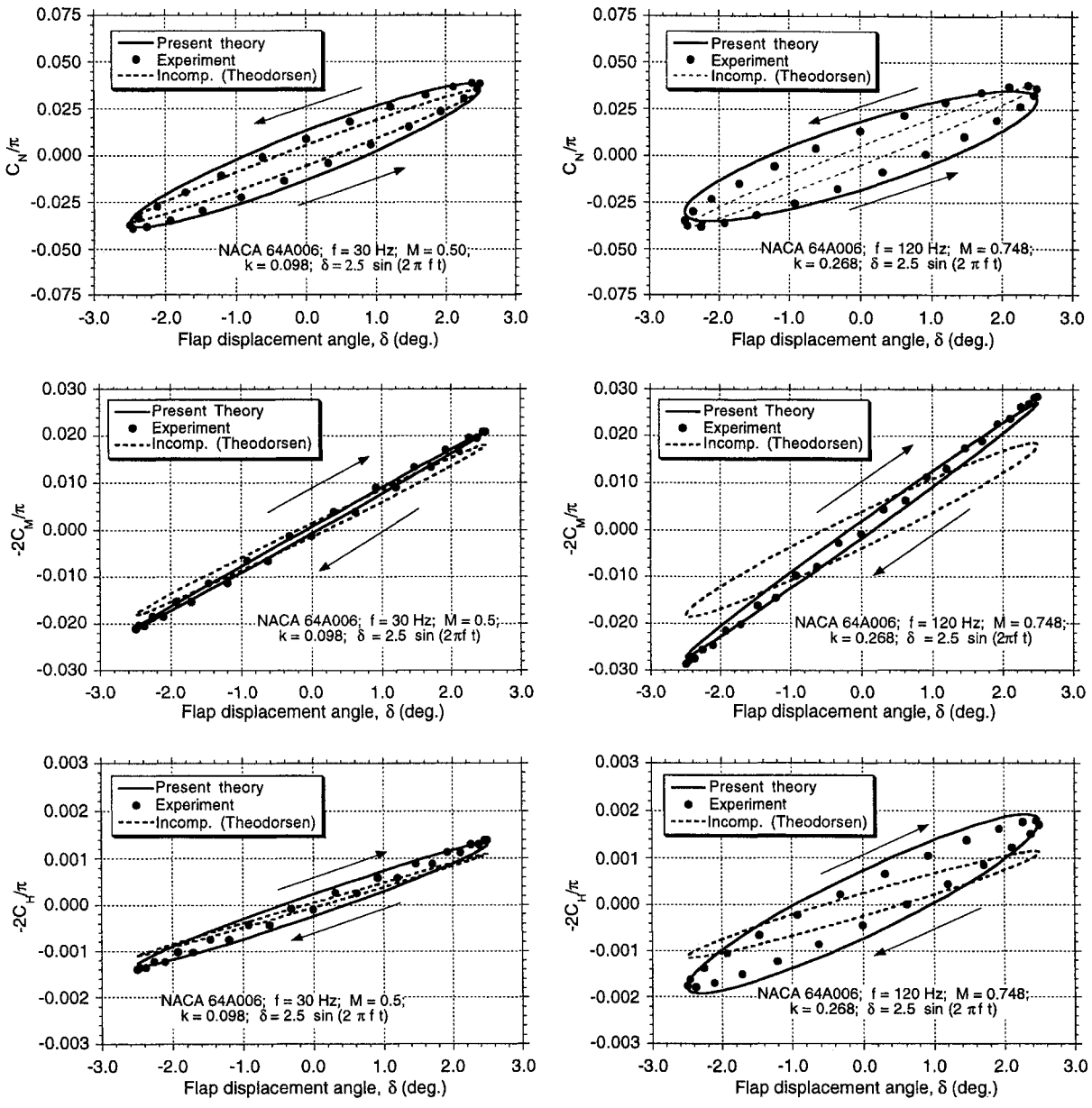

Fig. 11 Comparison of predicted lift, moment, and hinge moment vs flap deflection angle with experimental data for an oscillating flap motion at two Mach numbers.

Figure 11 shows that the airfoil moment behaves in an almost quasisteady manner, as discussed previously with regard to Fig. 9. Here, the moment loops are circumvented in a clockwise sense, but the phase lead is small. In general, there is a weak effect of both Mach number and frequency on the unsteady airfoil moment because of flap deflection, and would be adequately predicted in the general case if quasisteady conditions were assumed. On the other hand, the flap hinge moment shows a considerably more powerful unsteady effect. Here, there is a phase lead between the response and the forcing, giving loops that are circumvented in a clockwise direction. Again, this is because of the noncirculatory terms, which play a very important role in the response at higher flap frequencies. Clearly, these results dictate the use of a compressible flow theory to model the quantitative effects on the airloads.

Concluding Remarks

Indicial aerodynamic functions have been derived for trailing-edge flap displacement and flap angular rate motion in subsonic compressible flow. Exact values of the indicial normal force (lift) and moment about the one-quarter-chord were derived by using the aerodynamic reverse flow theorems in conjunction with the exact pressure distributions computed for the flat-plate case. These results were used to help obtain complete asymptotic approximations for the respective indicial responses. Approximations to the indicial response were also derived for the hinge moments. Thereafter, the normal force, airfoil moment, and hinge moment airloads because of arbitrary flap motion were obtained in state–space form.

Validation of the method has been conducted with experimental data for time-dependent (ramp) and oscillating flap motion at various subsonic Mach numbers. The agreement was found to be good, although some minor discrepancies in the predictions were noted at the higher Mach numbers. While nonlinear effects are likely responsible for these differences, it is clear that, bearing in mind the relative simplicity of the present method, the approach provides a good estimate of the aerodynamic forces and moments because of the unsteady deflection of a flap. Furthermore, these predictions appear superior to those obtained with classical unsteady incompressible theory, especially at higher freestream Mach numbers and reduced frequencies. However, further measurements at higher flap deflection amplitudes and/or mean AOAs are obviously required to fully explore the limitations of the present theory for more general use in a rotor analysis.

Acknowledgments

The first author was partially supported by the U.S. Army Research Office under Contract DAAL03-92-G-0121, Smart Structures Technology: Innovations & Applications to Rotorcraft Systems, Gary Anderson was the Technical Monitor.

References

[1]Edwards, J. W., "Flight Test Results of an Active Flutter Suppression System," *Journal of Aircraft*, Vol. 20, No. 3, 1983, pp. 267–274.

[2]Nissim, E., "Comparative Study Between Two Different Active Flutter Suppression Systems," *Journal of Aircraft*, Vol. 15, Dec. 1978, pp. 843–848.

[3]Millott, T. A., and Friedmann, P. P., "Vibration Reduction in Helicopter Rotors Using an Active Control Surface Located on the Blade," *Proceedings of the AIAA/ASME/ASCE/AHS/ASC 33rd Structures, Structural Dynamics, and Materials Conference*, AIAA, Washington, DC, 1992, pp. 1975–1988.

[4]Chen, P. C., and Chopra, I., "Development of an Intelligent Rotor," *Proceedings of the 4th Workshop on Dynamics and Aeroelasticity Modeling of Rotorcraft Systems*, Univ. of Maryland, College Park, MD, 1991.

[5]Dawson, S., and Straub, F., "Design, Validation and Test of a Model Rotor with Tip Mounted Active Flaps," *Proceedings of the American Helicopter Society 50th Annual Forum*, American Helicopter Society, Washington, DC, 1994, pp. 361–372.

[6]Bir, G., and Chopra, I., "University of Maryland Advanced Rotor Code (UMARC) Theory Manual," Center for Rotorcraft Education and Research, Univ. of Maryland, UM-AERO 92-02, College Park, MD, Nov. 1992.

[7]Rutkowski, M. J. (ed.), "2GCHAS Theory Manual," Dept. of the Army, Aeroflightdynamics Directorate, NASA Ames Research Center, Moffett Field, CA, Dec. 1990.

[8]Leishman, J. G., "Unsteady Lift of a Flapped Airfoil by Indicial Concepts," *Journal of Aircraft*, Vol. 31, No. 2, 1994, pp. 288–297.

[9]Van der Wall, B., and Leishman, J. G., "The Influence of Variable Flow Velocity on Unsteady Airfoil Behavior," *Journal of the American Helicopter Society*, Vol. 39, No. 4, 1994, pp. 25–36.

[10]Küssner, H. G., and Schwartz, L., "The Oscillating Wing with Aerodynamically Balanced Elevator," NACA Translation TM 991, Dec. 1940.

[11]Theodorsen, T., "General Theory of Aerodynamic Instability and the Mechanism of Flutter," NACA Rept. 496, 1935, pp. 413–433.

[12]Theodorsen, T., and Garrick, I. E., "Nonstationary Flow About a Wing-Aileron-Tab Combination, Including Aerodynamic Balance, NACA Rept. 736, 1942, pp. 129–138.

[13]Drescher, H., "Untersuchungen an einem symmetrischen Tragflügel mit spaltos angeschlossenem Ruder bei raschen Aenderungen des Ruderausschlags (ebene Strömung)," Max-Plank Inst. für Strömungsforschung, Göttingen, Germany, 1952.

[14]Bisplinghoff, R. L., Ashley, H., and Halfman, R. L., *Aeroelasticity*, Addison–Wesley, Reading, MA, 1955, pp. 281–293.

[15]Leishman, J. G., and Nugyen, K. Q., "A State-Space Representation of Unsteady Aerodynamic Behavior," *AIAA Journal*, Vol. 28, No. 5, 1990, pp. 836–845.

[16]Edwards, J. W., Ashley, H., and Breakwell, J. V., "Unsteady Aerodynamic Modeling for Arbitrary Motions," *AIAA Journal*, Vol. 17, No. 4, 1979, pp. 365–374.

[17]Beddoes, T. S., "A Synthesis of Unsteady Aerodynamic Effects Including Stall Hysteresis," *Vertica*, Vol. 1, No. 2, 1976, pp. 113–123.

[18]Leishman, J. G., and Beddoes, T. S., "A Semi-Empirical Model for Dynamic Stall," *Journal of the American Helicopter Society*, Vol. 34, No. 3, 1989, pp. 3–17.

[19]Hariharan, N., "Unsteady Aerodynamics of a Flapped Airfoil in Subsonic Flow Using Indicial Concepts," M.S. Thesis, Univ. of Maryland, College Park, MD, 1995.

[20]Hariharan, N., and Leishman, J. G., "Unsteady Aerodynamics of a Flapped Airfoil in Subsonic Flow Using Indicial Concepts," AIAA Paper 95-1228, April 1995.

[21]Lomax, H., "Indicial Aerodynamics," *AGARD Manual of Aeroelasticity*, Pt. II, Nov. 1960, Chap. 6.

[22]Leishman, J. G., "Validation of Approximate Indicial Aerodynamic Functions for Two-Dimensional Subsonic Flow," *Journal of Aircraft*, Vol. 25, No. 10, 1987, pp. 914–922.

[23]Leishman, J. G., "Indicial Lift Approximations for Two-Dimensional Subsonic Flow as Obtained from Oscillatory Measurements," *Journal of Aircraft*, Vol. 30, No. 3, 1993, pp. 340–351.

[24]Mazelsky, B., "On the Noncirculatory Flow About a Two-Dimensional Airfoil at Subsonic Speeds," *Journal of the Aeronautical Sciences*, Vol. 19, No. 12, 1952, pp. 848, 849.

[25]Beddoes, T. S., "Practical Computation of Unsteady Lift," *Vertica*, Vol. 8, No. 1, 1984, pp. 55–71.

[26]Mazelsky, B., "Determination of Indicial Lift and Moment of a Two-Dimensional Pitching Airfoil at Subsonic Mach Numbers from Oscillatory Coefficients with Numerical Calculations for a Mach Number of 0.7," NACA TN 2613, Feb. 1952.

[27]Mazelsky, B., and Drischler, J. A., "Numerical Determination of Indicial Lift and Moment Functions of a Two-Dimensional Sinking and Pitching Airfoil at Mach Numbers 0.5 and 0.6," NACA TN 2739, 1952.

[28]Lomax, H., Heaslet, M. A., Fuller, F. B., and Sluder, L., "Two and Three Dimensional Unsteady Lift Problems in High Speed Flight," NACA Rept. 1077, 1952, pp. 393–447.

[29]Flax, A. H., "Reverse-Flow and Variational Theorems for Lifting Surfaces in Nonstationary Compressible Flow," *Journal of the Aeronautical Sciences*, Vol. 20, No. 2, 1952, pp. 120–126.

[30]Heaslet, M. A., and Spreiter, J. R., "Reciprocity Relations in Aerodynamics," NACA Rept. 1119, 1953, pp. 253–268.

[31]White, R. B., and Landahl, M., "Effect of Gaps on the Loading Distribution of Planar Lifting Surfaces," *AIAA Journal*, Vol. 6, No. 4, 1968, pp. 626–631.

[32]Gray, R., and Davis, D. E., "Comparison of Experimentally and Theoretically Determined Values of Oscillatory Aerodynamic Control Surface Hinge Moment Coefficients," Royal Aircraft Establishment

TR 72023, March 1972.

[33]Tijdeman, H., and Schippers, P., "Results of Pressure Measurements on an Airfoil with Oscillating Flap in Two-Dimensional High Subsonic and Transonic Flow," National Aerospace Lab., The Netherlands, July 1973.

[34]Garrick, I. E., "Propulsion of a Flapping and Oscillating Airfoil" NACA Rept. 567, 1936.

[35]Leishman, J. G., "An Analytic Model for Unsteady Drag," *Journal of Aircraft*, Vol. 25, No. 7, 1988, pp. 665, 666.

[36]Fung, Y. C., *An Introduction to the Theory of Aeroelasticity*, Wiley, New York, 1955.

[37]Zwaan, R. J., "NACA 64A006, Oscillating flap," *A Compendium of Unsteady Aerodynamic Measurements*, edited by N. C. Lambourne, AGARD R-702, Aug. 1982.

[38]Zwaan, R. J., "NLR 7301 Supercritical Airfoil—Oscillatory Pitching and Oscillating Flap," *A Compendium of Unsteady Aerodynamic Measurements*, edited by N. C. Lambourne, AGARD R-702, Aug. 1982.